

# ECG Signal Data Classification System Based on Hankel Dynamic Mode Decomposition

Chuchu Liang<sup>a,b</sup>, Majid Khan Majahar Ali<sup>a\*</sup>, Lili Wu<sup>a</sup>, Zhixiang Zhang<sup>c</sup>

<sup>a</sup>School of Mathematical Sciences, Universiti Sains Malaysia, 11800 USM, Pulau Pinang, Malaysia; <sup>b</sup>School of General Studies, Shanxi Institute of Science and Technology, 048000 Jincheng, Shanxi, China; <sup>c</sup>School of Mathematics and Computer Science, Shanxi Normal University, 030000 Taiyuan, Shanxi, China

**Abstract** The modes in the electrocardiogram (ECG) signal can be divided into stable modes and unstable modes. The unstable modes are of great significance for signal analysis and classification. When the traditional dynamic mode decomposition (DMD) method is directly applied to these signals, it is difficult to effectively extract these key modes due to the rank mismatch problem of the data matrix. In order to better capture and analyze unstable modes, this study introduced the Hankel matrix to expand ECG data and used it as the input of DMD to propose the Hankel dynamic mode decomposition (HDMD) method. Although HDMD has been applied in other physiological signal processing, this study is the first to successfully apply it to multi-lead ECG signal analysis. By optimizing the delay parameters of the Hankel matrix and retaining the modes that account for 90% of the singular value decomposition energy, we significantly improve the effectiveness of feature extraction. Each type of abnormal ECG signal data is classified on the PTB Diagnostic ECG database. The experimental results of the proposed model are compared with the direct use of DMD for modal extraction. The highest classification accuracy of multi-modal ECG signal data extracted by HDMD is more than 10% higher than that using DMD. At the same time, the mean squared error (MSE) of the reconstruction using HDMD is 0.282 lower than that of DMD, indicating a significant improvement in reconstruction accuracy. Further illustrating the proposed method, the HDMD method can better capture and analyze the unstable modes in the ECG signal, thereby significantly improving the accuracy and robustness of signal classification. Future work will focus on further optimizing the parameter selection of the HDMD model and exploring its application potential in real-time heart disease monitoring and early warning systems.

**Keywords:** Hankel matrix, Hankel dynamic mode decomposition (HDMD), classifier, ECG signals.

**\*For correspondence:**  
majidkhanmajaharali@usm.  
my

**Received:** 15 Oct. 2024  
**Accepted:** 31 Dec. 2024

©Copyright Liang. This article is distributed under the terms of the [Creative Commons Attribution License](#), which permits unrestricted use and redistribution provided that the original author and source are credited.

## Introduction

The ECG signal stands as a record of cardiac activity, embodying a nonlinear signal, extensively utilized for the assessment of cardiac ailments [1]. Normal ECG signals reflect the electrical activity of the heart in a stable state. It consists of a series of typical waveforms, including P waves, QRS complex waves and T waves, as shown in Figure 1 (a). These waveforms correspond to the processes of atrial depolarization, ventricular depolarization and repolarization. In a standard 12-lead ECG, the shape and amplitude of the waveforms in each lead show a specific distribution pattern, as shown in Figure 1 (b). The PR interval, QRS interval and QT interval are stable in equal time intervals, showing the electrophysiological characteristics of a healthy heart. This regularity and stability of normal ECG signals provide a baseline reference for clinical diagnosis.

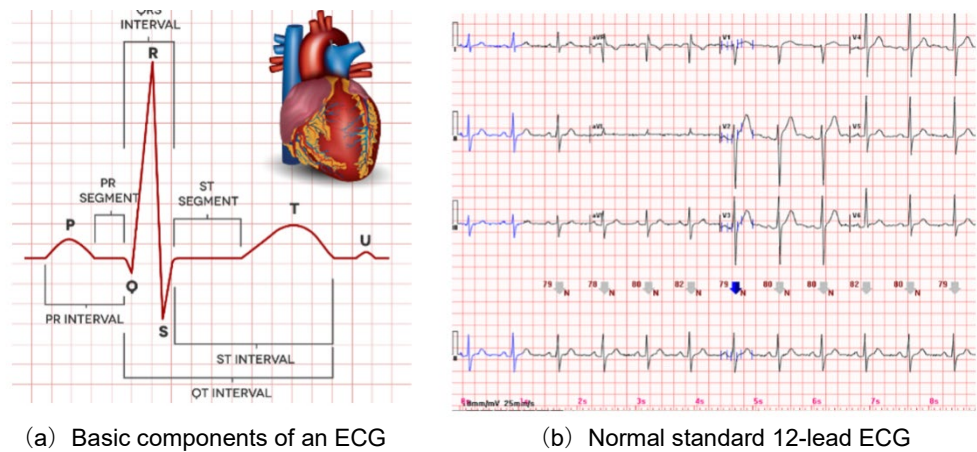


Figure 1. ECG components and normal 12-lead ECG

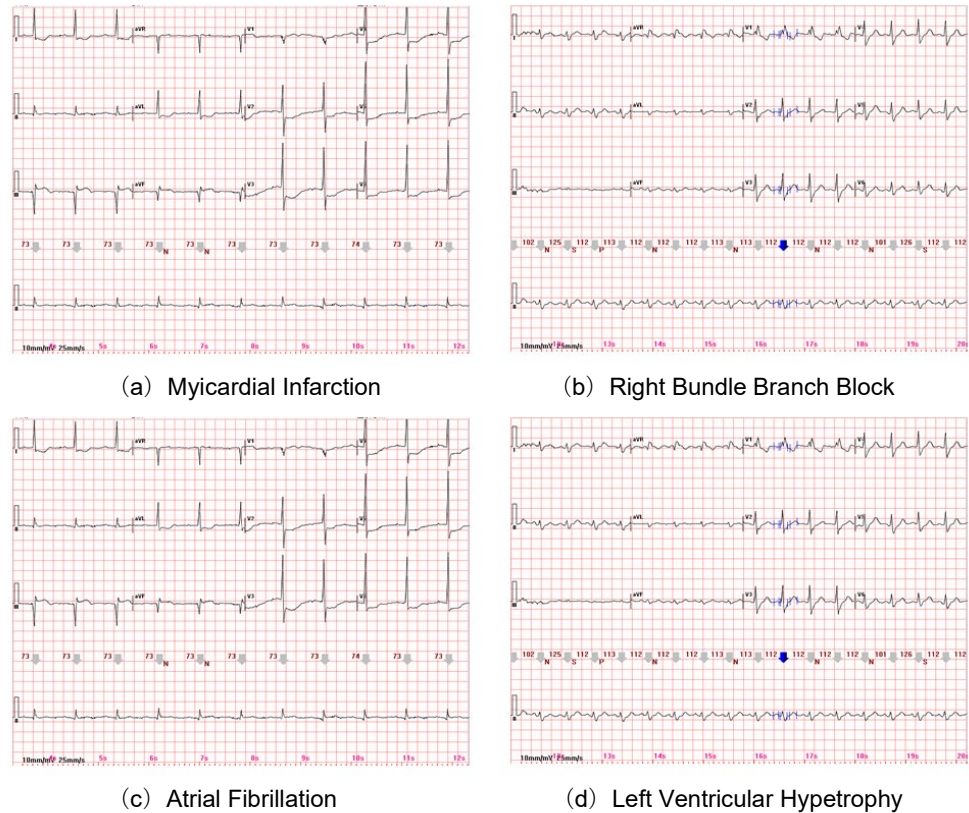
Abnormal ECG signals indicate pathological changes in cardiac function, often accompanied by abnormal waveforms, rhythms, or intervals. Table 1 summarizes in detail the key ECG features of seven heart diseases [2], including Myocardial Infarction, Cardiomyopathy, Bundle Branch Block, and Dysrhythmia, etc. In particular, Figure 2 specifically shows the abnormal parts of the ECG for four common diseases, including Myocardial Infarction (MI), Right Bundle Branch Block (RBBB), atrial fibrillation, and Left Ventricular Hypertrophy (LVH). These abnormal waveforms reflect the impact of various diseases on cardiac electrical activity and are an important basis for identifying and diagnosing these heart diseases. If different heart diseases can be effectively classified based on ECG signal data [3], it will help doctors detect and deal with abnormal conditions on time and keep patients' hearts healthy. In addition, the appearance of abnormal signals is usually associated with unstable modes, which can reveal underlying pathological processes and become an important basis for disease diagnosis and treatment.

Table 1. Summary of ECG characteristics of various heart diseases

No.	Cardiac Diseases	ECG Characteristics
1	Myocardial Infarction	ST-segment elevation or depression, pathological Q waves (deepened, widened), inverted T waves.
2	Cardiomyopathy/Heart Failure	Low voltage QRS complex, abnormal T waves (flattened or inverted), prolonged QRS duration, possible bundle branch block or atrial fibrillation.
3	Bundle Branch Block	Right Bundle Branch Block (RBBB): Wide QRS complex with an "M" pattern in V1, deep S wave in V6. Left Bundle Branch Block (LBBB): Wide QRS complex, QS wave (or small r wave) in V1, broad and notched R wave in V6
4	Dysrhythmia	Absent P waves (atrial fibrillation), wide QRS complex (premature ventricular contractions), bradycardia, or tachycardia.
5	Myocardial Hypertrophy	Right Ventricular Hypertrophy (RVH): Tall R wave in V1, deep S wave in V6. Left Ventricular Hypertrophy (LVH): High QRS voltage, deep S wave in V1, tall R wave in V5/V6.
6	Valvular Heart Disease	Widened and notched P waves (mitral stenosis), characteristic QRS changes indicating left ventricular hypertrophy (aortic stenosis).
7	Myocarditis	Flattened or inverted T waves, non-specific ST segment changes (elevation or depression), prolonged PR interval, possible arrhythmias.

DMD emerges as a mathematical technique for extracting dynamic modes from time series data [4]. It decomposes time series data into a series of spatial modes and corresponding temporal modes, thereby capturing dynamic features and structural information within the data. Employing extracted dynamic modes for ECG data classification enhances algorithmic operational efficiency. DMD obviates the need for physical modeling of systems, instead directly extracting dynamic information from data, thus being suitable for various complex systems [5]. With a relatively straightforward computational process, typically involving basic operations such as matrix computations and eigenvalue decomposition, DMD boasts high computational efficiency [6]. Each mode corresponds to a dynamic feature within the data,

facilitating convenient data interpretation and analysis. DMD not only finds utility in the decomposition and analysis of time series data but also extends its application to domains such as image processing, fluid mechanics, and dynamic systems [7]-[8]. Despite its numerous advantages, DMD does possess limitations, including a higher requirement for data linearity and relatively weaker handling capabilities for noise and non-linear effects [9]. Hence, the application of DMD necessitates prudent selection and adjustments based on the specific characteristics of the problem at hand.



**Figure 2.** ECG characteristics of typical heart diseases.

However, in ECG signal analysis, the stability of the modes is a key issue. The modes in the ECG signal can be divided into stable modes and unstable modes [10]. This study focuses more on unstable modes because the changes in these modes can indicate underlying cardiac pathologies and provide key physiological information for diagnosis and treatment. Unstable modes, especially in abnormal conditions such as heart attacks or other acute cardiac events, often exhibit more complex dynamic characteristics. Traditional DMD methods often encounter the problem of data matrix rank mismatch when processing these signals, that is, the number of rows is much smaller than the number of columns, which causes DMD to be ineffective in extracting mode features.

The objective of this study is to improve DMD. Instead of extracting dynamic modes directly from the data, the Hankel matrix of ECG signal data is first constructed [11] and the DMD method is applied to extract the modes of the Hankel matrix. The delay parameters of the Hankel matrix are optimized and the modes that account for 90% of the singular value decomposition energy are retained. Hankel matrices preserve the temporal sequence structure of the original data, typically exhibiting superior numerical stability as they are constructed through sliding windows of the original data [12]. This approach aims to reduce computational complexity, enhance stability, and broaden applicability.

The research on ECG signal data classification primarily encompasses methods for feature extraction and optimization of various classification algorithms. The domain of feature extraction, it involves extracting both temporal and spectral features, which can be augmented through signal translation, scaling, and other techniques to enhance generalization capabilities. Among these techniques, the utilization of Hankel matrices for data transformation stands out as an effective method for data augmentation. Sun *et al.* proposed an enhanced method based on Hankel matrices for identifying states

based on the vibrations sampled at each rotation of the main axis, with matrix similarity employed for mechanical operation state monitoring [12]. Frolov *et al.* employed a method based on specialized Hankel matrices to replicate certain properties of self-attention networks, significantly accelerating training time and demonstrating competitiveness in recommendation quality [13]. Orinaitè *et al.* utilized rank measurement of Hankel matrices for feature extraction of ECG signals, combined with CNN for data classification [14]. Sharma *et al.* applied eigenvalue decomposition based on Hankel matrices to mitigate baseline drift and powerline interference in ECG signals, showcasing their effectiveness in time series preprocessing [15].

The Hankel matrix-based DMD modal extraction method has been employed in various fields for modal extraction. Curtis *et al.* leveraged the fundamental insights of the Takens embedding theorem to devise an adaptive learning scheme, proposing Deep Learning Hankel DMD for better approximation of high-dimensional and chaotic dynamics [16]. Kato *et al.* utilized this model for data-driven spectral analysis of access-restricted quantum spin networks [17]. Yang *et al.* introduced Hankel matrices to rearrange measurement data, harnessing the extended functionality of Hankel blocks to estimate modal frequencies and damping ratios with shorter data windows, thereby effectively reducing computational time. Simulated data from the IEEE 4-generator system and the IEEE 16-generator system along with real data were employed for training and testing [18]. Wang *et al.* employed the Hankel DMD method using synchronized phasor data to identify parameters of subsynchronous resonance (SSR) [19]. Nayak *et al.* proposed a data-driven reduced-order model (ROM) based on Hankel-DMD for rapid analysis and extrapolation of temporal electromagnetic responses in resonant cavities [20]. It is evident that the Hankel DMD model has found applications in numerous industries, yet currently, there exists no literature utilizing this model for ECG signal data classification systems. The core of HDMD lies in how to choose the appropriate delay parameters. The delay parameter selection of the Hankel matrix is to adjust the shape of the matrix to make it closer to “a square” or more “wide and fat” [21]. The optimization of the matrix shape can better preserve and capture the spatiotemporal patterns in the signal; minimize information loss in signal processing, especially when processing complex or nonlinear signals; and improve the numerical stability of subsequent calculation processes, especially in algorithms such as DMD. Although the Hankel DMD model has been applied to many industries, there is currently no relevant literature on the use of this model in ECG signal data classification systems.

Existing techniques still exhibit certain limitations:

(1)The extraction of features from ECG signals has not yet reached standardization, leading to inconsistencies in the methods used for feature extraction across different studies or applications, thereby diminishing the comparability and universality of these methods.

Presently, feature extraction methods are often coupled with subsequent classification or recognition tasks, a coupling that may result in limitations in the feature extraction method's ability to fully exploit the information within the signal.

(2)Directly employing DMD for mode extraction from ECG signals lacks thorough exploration of nonlinear temporal features and requires prior determination of the number of modes to be extracted, posing potential challenges to the stability of these modes.

(3)The imbalance in categories within ECG signal data results in poorer recognition performance for minority categories by classifiers. While deep learning models demonstrate remarkable performance in ECG signal classification, their internal workings and decision-making processes are challenging to elucidate, thereby diminishing the model's credibility and interpretability.

This study employs the HDMD method to enhance ECG signal data using Hankel matrices, utilizes DMD for mode extraction from Hankel matrices, further classifies the mode data, and enables data reconstruction. Compared to directly applying DMD to extract modes from the original signal, this approach better captures both temporal and spatial features of the data, thus benefiting classification efforts.

The main contributions of this manuscript can be summarized as follows:

(1)HDMD was first successfully applied to multi-lead ECG signal analysis, significantly improving the ability to capture unstable modes and the accuracy of signal classification.

(2)When performing singular value decomposition of Hankel matrices, the selection of the number of singular values, employing a proportion above 90% of singular values, consequently determines the number of extracted modes.

(3) Utilizing the inverse Hankelization operator for reconstructing the original data, revealing a smaller reconstruction error compared to direct employment of DMD.

(4) Conducting classification experiments on publicly available 12-lead ECG datasets with the proposed model and DMD. The experimental results indicate superior classification performance of our proposed model on this dataset.

## Methods

Figure 3 shows the specific algorithm flow. In this study, we proposed an ECG signal classification algorithm that combines the DMD technology with the Hankel matrix. First, the original ECG signal is preprocessed to remove noise and standardize the data. Next, the Hankel matrix is constructed to capture the timing characteristics of the signal, and the appropriate delay parameters are selected to optimize the representation ability of the matrix. Subsequently, the HDMD technology is applied to extract patterns with spatiotemporal dynamic characteristics. In order to verify the effectiveness of the proposed method, the extracted features are input into the support vector machine (SVM) classifier for classification, and the performance of the traditional DMD method and the HDMD method in SVM classification are compared. The accuracy and efficiency of the two in the ECG signal classification task are evaluated to demonstrate the superiority of HDMD in processing ECG signals and emphasize the potential advantages of HDMD in practical applications.

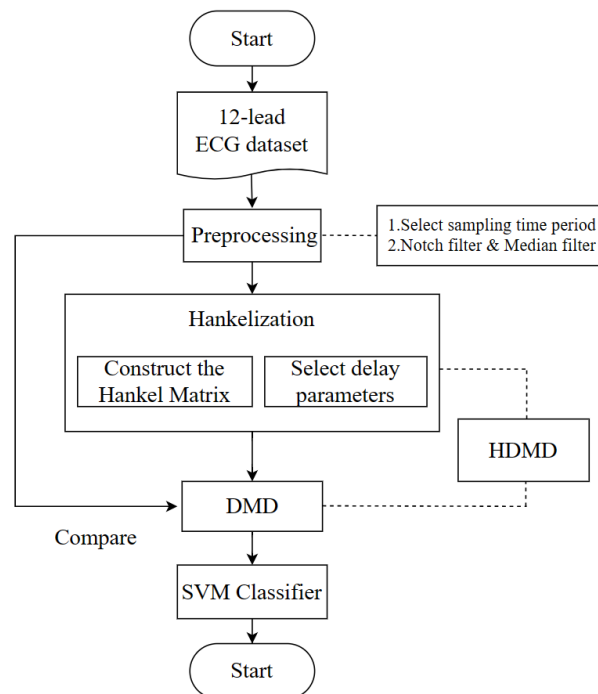


**Figure 3.** General overview diagram of the method

## ECG Dataset

The dataset is sourced from the PTB Diagnostic ECG database [22], renowned as one of the cardinal repositories for medical inquiry into electrocardiographic data. It encompasses a spectrum of pathological conditions including normal sinus rhythms, myocardial infarctions, left ventricular hypertrophies, myocardial ischemias, and beyond. This compendium comprises ECG recordings from 290 subjects, each delineated by one to five records. Notably absent are subjects numbered 124, 132, 134, and 161. Each recording encapsulates 15 concurrently measured signals: the conventional 12 leads (i, ii, iii, avr, avl, avf, v1, v2, v3, v4, v5, v6) alongside 3 Frank leads (vx, vy, vz). Each signal is digitized at a velocity of 1000 samples per second, with a resolution of 16 bits within the range of  $\pm 16.384$  mV. Clinical summaries for 22 subjects are void, hence not enlisted for analysis. The diagnostic categories for the remaining 268 subjects are elucidated in Table 2.

**Table 2.** The diagnostic classes of the ECG dataset

class	Diagnostic class	Number of subjects
0	Healthy Controls	52
1	Myocardial Infarction	148
2	Cardiomyopathy/Heart Failure	18
3	Bundle Branch Block	15
4	Dysrhythmia	14
5	Myocardial Hypertrophy	7
6	Valvular Heart Disease	6
7	Myocarditis	4
8	Miscellaneous	4

The four entries in the Miscellaneous category encompass Palpitation, Stable angina, and Unstable angina. There are primarily eight categories, along with a set of healthy control counterparts labeled as 0, totaling 52 patients. Disparities exist in the volume of data across each diseased category, with myocardial infarction boasting the highest count at 148 entries. This article will conduct a classification study by juxtaposing ECG signal data from each Diagnostic class with the Healthy Controls group, thereby contrasting the classification efficacy extracted by the DMD method.

### Data Preprocessing

In the process of signal or data analysis, particularly when dealing with biomedical signals, time series data, or any form of continuous signals, the efficacy of preprocessing steps is pivotal for an accurate understanding and analysis of such data [23]-[24]. This preprocessing primarily encompasses two crucial components: the selection of sampling intervals and the removal of denoising and baseline drift from the signal. These two steps play a paramount role in enhancing the accuracy and reliability of data analysis.

The selection of sampling intervals entails determining which time periods of the data should be considered in the analysis, a process typically reliant on the characteristics of the signal and the objectives of the analysis. In ECG signal data, the concept of spectral peaks holds significant importance [25], as for some strongly periodic signals, their spectra often contain prominent peaks. These peaks correspond to the major cycles within the signal and also align with the principal dynamic modes in DMD. Analogous to the beat segmentation of R-waves discussed in [10], the sampling intervals are determined based on the peaks following the R-wave.

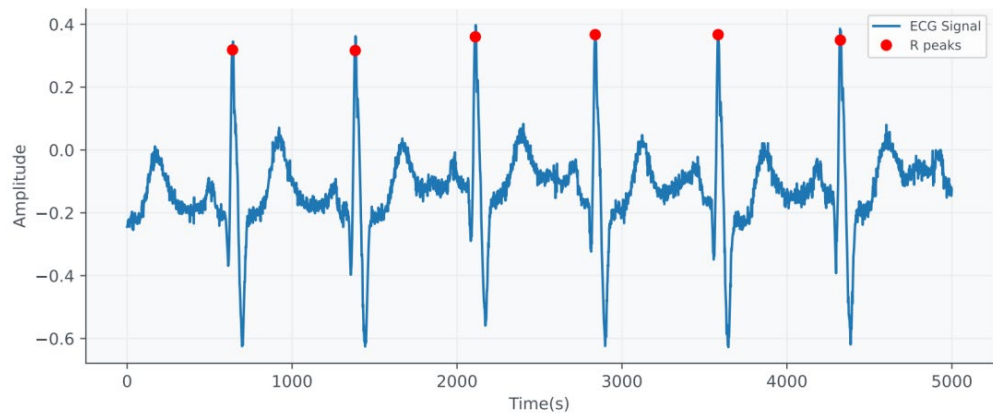


**Figure 4.** ECG Signal with R peaks

Figure 4 delineates the precise locations of the R peaks among the first 5000 sampling points on a lead, revealing a total of six discernible R peaks. Correspondingly, Table 3 delineates the inter-peak distances between adjacent R peaks within the initial 5000 sampling points across twelve leads for a patient. (Here, the sampling frequency is 1000Hz, with distances measured in sampling points.)

Table 3 shows that there are up to 745 sampling points between adjacent R peaks. Consequently, this paper opts for 750 sampling points. The first R peak occurs around 640-time points, while the second occurs approximately at 1385. Utilizing the second beat data, analysis will encompass sampling points between 1236 and 1985, comprising 150 data points before and 600 data points after the R peak.

**Table 3.** Number of sampling points between adjacent R peaks

No.	R1-R2	R2-R3	R3-R4	R4-R5	R5-R6
1	744	728	727	745	741
2	744	728	727	745	741
3	744	728	727	745	742
4	745	730	726	744	742
5	744	727	727	745	741
6	744	728	727	745	741
7	746	729	725	744	744
8	744	727	728	745	741
9	744	727	728	745	741
10	743	728	728	745	740
11	743	729	727	745	741
12	744	729	727	744	742

Preprocessing of ECG signals stands as a pivotal stride, considering all potential sources of noise, such as motion artifacts and power line interference, which could impede the subsequent model's performance. Therefore, in this paper, the following two-step preprocessing is applied to the ECG signals:

(1) Notch filtering

Mitigating power supply interference precedes subsequent low-pass filtration to eliminate high-frequency noise. Notch filtering primarily targets the elimination of specific frequency interference signals, employing the Infinite Impulse Response (IIR) filter herein [26]:

$$x_n = y_n - a_1x_{n-1} - a_2x_{n-2}. \tag{1}$$

Where,  $y_n$  represents the input ECG signal, while  $x_n$  represents the filtered ECG signal. The coefficients  $a_1$  and  $a_2$  are determined based on the center frequency and bandwidth of the notch filter.

(2) Median filtering

By substituting the value of the current data point with the median of the data within the filtering window, it effectively attenuates noise in the signal while preserving its clarity [27]. Given a signal  $x_n$  to be filtered, with a window length set to  $L$ , the filtered signal is denoted as  $\hat{x}_n$ .

For the  $i$ -th data point, a window containing the  $i$ -th data point, with a length of  $L$ , is chosen. The  $L$  data points within the window are sorted in ascending order, and then the median value is selected as the filtering result for the  $i$ -th data point:

$$\hat{x}_i = M\left(x_{i-\frac{L-1}{2}}, x_{i-\frac{L-1}{2}+1}, \dots, x_{i+\frac{L-1}{2}}\right) \tag{2}$$

Where,  $M$  represents the operation of taking the median,  $i \in \left(\frac{L-1}{2}, N - \frac{L-1}{2}\right)$ , and  $N$  represents the length of the data. When the window size is set to 1, the median filter degenerates into a situation where no filtering is performed,  $\hat{x}_n = x_n$ .

**Construct Hankel Matrix of ECG Signals**

We shall denote the ECG data collected from  $N$  leads at timestamp  $t$  as  $x_t \in R^N$  ( $t = 1, 2, \dots, T$ ). The entire dataset is represented as:

$$X_T = \begin{pmatrix} x_{1,1} & \dots & x_{1,T} \\ \vdots & \ddots & \vdots \\ x_{n,1} & \dots & x_{n,T} \\ \vdots & \ddots & \vdots \\ x_{N,1} & \dots & x_{N,T} \end{pmatrix} = [x_1, \dots, x_t, \dots, x_T] \tag{3}$$

Each row is denoted as  $x_n$ , representing the data collected at  $T$  time points on the  $n$ -th lead and  $X_T \in \mathbb{R}^{N \times T}$ . Here  $T$  equals 750, while  $N$  equals 12. Assuming the ECG system functions as a localized linear dynamic system, hence  $x_{t+1} = Ax_t$ , where  $A \in \mathbb{R}^{N \times N}$  represents the dynamics system [18].

DMD aims to compute the principal characteristic decomposition of the optimal fitting matrix  $A$  for all electrocardiogram (ECG) signal data  $X$ . However, in ECG signal data, where  $N = 12$ , significantly smaller than  $T$ , there arises a severe rank mismatch issue. Hankelization, on the other hand, emerges as a valuable technique for data augmentation, enabling recursive enhancement of data by replicating portions of it [28]. Consequently, we construct a Hankel matrix  $H$  to augment the dimensions of the data. Given the embedding delay length  $M$ , we can construct  $H$  from  $X$  through Hankelization operations. Firstly, for each row of  $X_T$ , representing the ECG signal data  $x_n$  on the  $n$ -th lead of the patient, we construct the corresponding Hankel matrix:

$$H_1^n = \begin{pmatrix} x_{n,1} & x_{n,2} & \cdots & x_{n,T-M+1} \\ x_{n,2} & x_{n,3} & \cdots & x_{n,T-M+2} \\ \vdots & \vdots & \ddots & \vdots \\ x_{n,M} & x_{n,M+1} & \cdots & x_{n,T} \end{pmatrix}^T_{M \times (T-M+1)} \tag{4}$$

and

$$H_2^n = \begin{pmatrix} x_{n,2} & x_{n,3} & \cdots & x_{n,T-M+2} \\ x_{n,3} & x_{n,4} & \cdots & x_{n,T-M+3} \\ \vdots & \vdots & \ddots & \vdots \\ x_{n,M+1} & x_{n,M+2} & \cdots & x_{n,T+1} \end{pmatrix}^T_{M \times (T-M+1)} \tag{5}$$

Similarly, we can obtain  $H_2^n = A_H H_1^n$ . Then rearrange the Hankel matrices on each lead to obtain a new matrix:

$$H_1 = [H_1^1, H_1^2, \dots, H_1^N]^T \in \mathbb{R}^{MN \times (T-M+1)} \tag{6}$$

and

$$H_2 = [H_2^1, H_2^2, \dots, H_2^N]^T \in \mathbb{R}^{MN \times (T-M+1)} \tag{7}$$

By utilizing  $H_1$  and  $H_2$  as inputs to DMD, the problem of DMD modal extraction transforms into the quest for the eigenvalues and eigenvectors of  $A_H$  in the equation below [28]:

$$H_2 = A_H H_1 \tag{8}$$

### Hankel Dynamic Mode Decomposition (HDMD)

It is evident that the parameter  $M$ , as elucidated by [20], delineates the dimensions of the Hankel matrix, consequently shaping the organization of time-series data into said matrix, thus impacting the subsequent quality and efficacy of the DMD model. Nevertheless, the determination of the delay parameter often occurs post DMD modal extraction from the Hankel matrix, prompting a simultaneous consideration of various delay parameter effects during singular value extraction to ascertain said parameters. The specific procedural diagram is depicted in Figure 5:

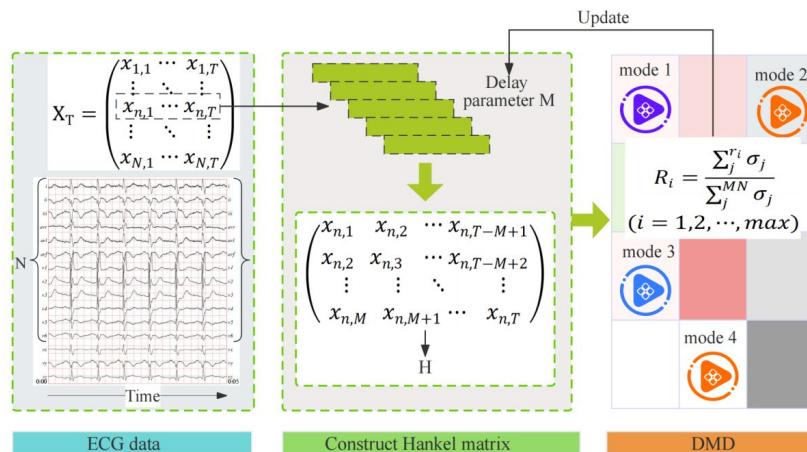


Figure 5. HDMD model framework

According to Equation (8), the optimal approximation operator  $A_H$  can be represented as:

$$A_H = H_2 H_1^\dagger \tag{9}$$

The symbol  $\dagger$  denotes the Moore-Penrose pseudoinverse of the matrix. The dynamic modal eigenvectors reflect spatial correlations, with each eigenvector determined by its corresponding eigenvalue. However, direct analysis of  $A_H$  proves to be challenging. Instead, DMD employs singular value decomposition to project the matrix  $A_H$  onto a low-rank space, extracting the primary eigenvalues and eigenvectors of  $A_H$  from a rank-reduced matrix, denoted by  $\tilde{A}_H$ . The specific steps are as follows:

Step1: Conduct singular value decomposition (SVD) on  $H_1$  [29]:

$$H_1 = U \Sigma V^* \tag{10}$$

Receive matrices  $U$ ,  $\Sigma$ , and  $V$ , where  $\Sigma$  denotes a diagonal matrix composed of singular values, denoted as  $\Sigma = \text{diag}(\sigma_j)$ ;  $V^*$  is the lower triangular matrix, being the conjugate transpose of  $V$ ;  $U$  is the upper triangular matrix,  $U^* U^T = V^* V^T = I$ , and  $I$  represents the identity matrix.

Step2: Calculate the pseudo-inverse of  $H_1$  using formulas (7) and (8) to obtain the matrix  $A_H$ :

$$A_H = H_2 V \Sigma^{-1} U^* \tag{11}$$

where  $\Sigma^{-1}$  represents the inverse of  $\Sigma$ .

Step 3: The mapping of  $A_H$  onto a lower-dimensional subspace, denoted as  $\tilde{A}_H$ , is defined as follows:

$$\tilde{A}_H = U_r^* A_H U_r = U_r^* A_H V_r \Sigma_r^{-1} \tag{12}$$

The parameter  $r$  denotes the rank of matrix  $A_H$ , thereby governing the eventual number of modes extracted. The selection of  $r$  is determined by the singular values of  $\Sigma$ , which is obtained through the singular value decomposition of the Hankel matrix. This process is influenced by the lag parameter  $M$ . Hence, the determination of  $M$  and  $r$  relies on whether the singular value ratio (SVR) meets the specified threshold.

$$R_i = \frac{\sum_j^{r_i} \sigma_j}{\sum_j^{MN} \sigma_j} \quad (i = 1, 2, \dots, \text{max}) \tag{13}$$

The  $i$ -th delay parameter has been selected, where  $r_i$  denotes the number of singular values reached when the threshold  $\delta$  ( $\delta = 90\%$ ) is attained.  $R_i$  represents the ratio of the first  $r_i$  singular values, with  $\text{max}$  denoting the maximum delay parameter set.

Step4: Computation of the Eigenvalue Decomposition:

$$\tilde{A}_H W = W \Lambda \tag{14}$$

where matrix  $\Lambda$  represents a diagonal matrix with its diagonal elements being the eigenvalues  $\lambda_k$  of matrix  $\tilde{A}_H$ . Matrix  $W$  consists of the eigenvectors of  $\tilde{A}_H$ , where each column corresponds to the eigenvector of  $\lambda_k$ .

Step5: The eigen decomposition of matrix  $A_H$  is constructed by  $W$  and  $\Lambda$ , where the DMD eigenvalues  $\Lambda$  are provided, and the modal matrix  $\Phi_H$  is composed of the eigenvectors of matrix  $A_H$  [30]:

$$\Phi_H = H_2 V \Sigma^{-1} W \tag{15}$$

These modes represent the eigenvectors of the high-dimensional operator  $A_H$ , where each mode  $\phi_k$  corresponds to an eigenvalue  $\lambda_k$  of  $\Lambda$ .

Step6: ECG signal data from other temporal-spatial domains can be approximated into a simplified dynamic model  $\hat{H}$ :

$$\hat{H} = \sum_{k=1}^r \phi_k e^{\omega_k t} b_k \tag{16}$$

where  $\omega_i = \ln(\lambda_k) / \Delta t$ , the modal amplitude  $b_k = \Phi_H^\dagger h_1$  stands for the initial amplitude of each modal order.  $H_1$  represents the first column of the Hankel matrix, denoting the spatial domain at the initial moment ( $t = 0$ ).  $r$  indicates the number of extracted modes, thus forming the reconstruction matrix  $\hat{H}$  for Hankel matrix  $H_1$ .

Step7: Employ the inverse Hankelization operator to transition  $\hat{H}$  to  $\hat{X}$ , thereby obtaining the reconstruction of  $X$  under the framework of HDMD.

### Evaluation Metrics

To ascertain the superior accuracy and efficacy of HDMD over conventional DMD modal extraction, SVM is employed to classify the extracted modal data and reconstructed data. Following preprocessing such as filtering, DMD and HDMD modal extraction are performed, and data reconstruction is conducted, contrasting the Reconstruction Mean Squared Error (MSE) [31]:

$$MSE = \frac{1}{N} \sum_{n=1}^N \|X_n - \hat{X}_n\| \tag{17}$$

where  $\|\cdot\|$  is Euclidean norm.

Utilizing Python-WFDB to acquire ECG signal data, gathered in temporal sequences, entails setting the sampling frequency to 1/1000 seconds for enhanced accuracy. Consequently, the acquired dataset size amounts to (268, 750, 12). Within this study, the ECG dataset encompasses solely 268 viable samples, comprising 8 categories of anomalies. One category, denoted as the Healthy Controls group, encompasses 52 patient samples. Each anomaly category is juxtaposed with the Healthy Controls group for classification.

In the evaluation of classification results, metrics including Accuracy (A), Precision (P), Recall (R), and F1 score (F1) are contrasted for each group. The respective formulae for these metrics are delineated in Table 4 where FP signifies instances where normal samples are erroneously classified as anomalies, leading to false positives. Conversely, FN denotes instances where anomaly samples are inaccurately classified as normal, resulting in false negatives. Similarly, TP and TN represent accurate identification of anomaly and normal instances, respectively.

**Table 4.** Confusion matrix for binary classification

No.	Actual\Predict	Positive	Negative
1	Positive	TP	FN
2	Negative	FP	TN

Different metrics can be evaluated as follows:

$$A = \frac{TP+TN}{TP+TN+FP+FN} \tag{18}$$

$$P = \frac{TP}{TP+FP} \tag{19}$$

$$R = \frac{TP}{TP+FN} \tag{20}$$

$$F1 = 2 \times \frac{P \times R}{P+R} \tag{21}$$

## Experiment Results

### Experimental Setup

The study employs data from 268 patients' ECG signals to train and validate the proposed model. All experiments were conducted using Python, utilizing the WFDB library for reading, writing, and processing ECG signal data, employing the sklearn machine learning library to instantiate various classification models, and leveraging BioSPPy for R-wave peak detection. All experiments were executed on a Windows 11 Pro 64-bit operating system, equipped with an Ultra 7 155U multicore processor clocked at 3.10 GHz.

### Delay Parameter Selection

The sampling frequency is 1/1000 seconds, and ECG data is processed through notch filtering and median filtering. Set the maximum delay parameter to max, then iterate the delay parameter  $M$  from 1 to max. Depending on the size of the ECG signal data (12,750), the corresponding Hankel matrix is of size  $(12M, 751 - M)$ . To reduce computational complexity,  $M$  is chosen within the range where  $12M < (751 - M)/2$ , implying  $\max \leq 30$ . Upon each iteration, the SVD decomposition of the Hankel matrix is performed, and the number of singular values contributing to 90% ratio shifts with  $M$ .

In Figure 6, the abscissa is the number of delay parameters, and the ordinate is the number of singular values when the SVR reaches 90%. As the delay parameter increases, the number of SVR required to reach 90% increases, indicating that as the delay parameter increases, the SVR decreases. Then we need to select more singular values, which will cause the Hankel matrix to be larger, increase the number of selected modes, and increase the computational complexity. Therefore, the delay parameter cannot be chosen too large. The optimal delay parameter is 25. At the same time, according to  $R_i > 90\%$ , the number of singular values here is  $r$ , that is, the low-dimensional representation of  $A_H$  is the rank of  $\tilde{A}_H$ , which is also the final mode number.

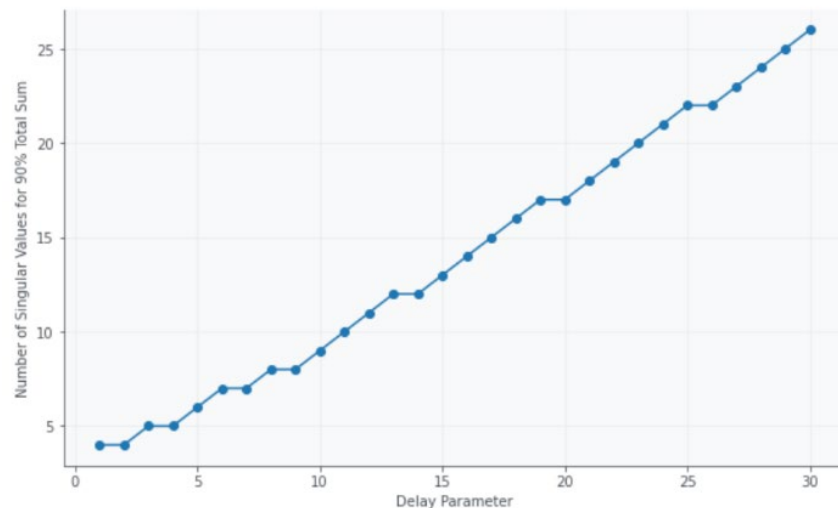


Figure 6. 90% SVR vs. Delay Parameter

Figure 7 is about the singular value distribution of a patient's 12-lead ECG signal data preprocessed and then directly subjected to singular value decomposition and Hankel matrix. Fig. 7 shows that the filtered ECG signal data is directly subjected to singular value decomposition. The distribution of singular values is relatively discrete, and the ratio of the first four singular values reaches 90%. Then the extracted modal vectors are also 4, which cannot be completely extracted. The original information of the data will inevitably have large errors when reconstructing the data on this basis, which will further affect the accuracy of classification. When performing singular value decomposition on the Hankel matrix constructed from filtered data, the singular value distribution falls smoothly, so that the information of the data can be obtained more comprehensively and stably. Moreover, the natural ratio reaches 90% at the 22nd singular value. In this way, the extracted modal vectors are 22, which can comprehensively obtain the changing trend of the data

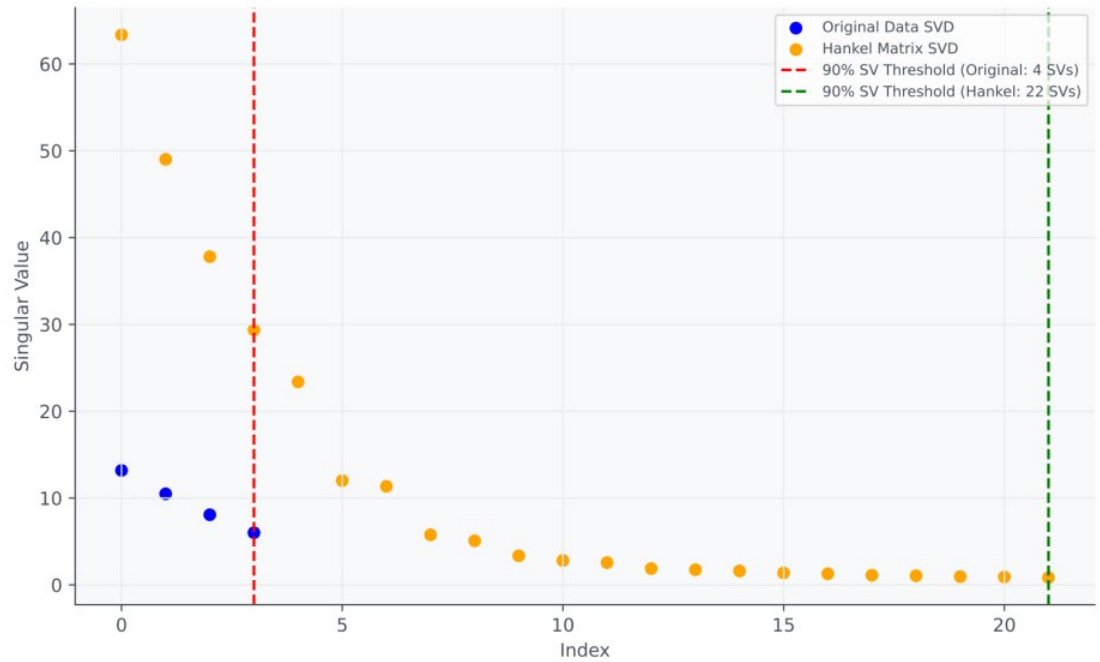


Figure 7. Comparison of Singular Value Distribution Between DMD and HDMD for ECG Data

We can also further illustrate that HDMD is more conducive to modal extraction of ECG signal data than DMD by comparing their reconstruction errors. Table 5 extracts the 12-lead data of a patient from 9 categories (detailed categories in Table 1) of ECG signal data, and uses DMD and HDMD for modal extraction and data reconstruction. Calculate the mean square error according to Equation (17), and intercept the singular values at the same position, that is, the same mode number  $r$ . It can be seen that among the 9 categories, except for the 7th category Myocarditis, the HDMD reconstruction error is smaller than the DMD reconstruction error, indicating that it is necessary to use the Hankel matrix for mode extraction in ECG signal processing.

Table 5. Confusion Matrix For binary classification

No.	MSE	0	1	2	3	4	5	6	7	8
1	DMD	0.446	0.044	0.156	0.077	0.138	0.100	0.192	0.160	0.052
2	HDMD	0.164	0.036	0.148	0.074	0.062	0.056	0.076	0.822	0.050

### Analysis of Classification Results

DMD and HDMD combined with SVM will be used to classify the modal data of the extracted ECG signal data, and the extracted modal data is complex numbers. In the experiment, the real part and imaginary part of each data are analyzed together, and each type of ECG is compared. Signal classification Accuracy, Precision, Recall, F1 score.

Each class is classified together with the health control class (Class 0). When using SVM for classification in the experiment, 0.8 is used as the training set. Because the number of patients is small, the verification set uses all data. Fig. 8 shows the confusion matrix heat map of HDMD and DMD classification, which intuitively displays the classification results of the classifier, and the classification situation of each category, including the number of correct classifications and incorrect classifications [32].

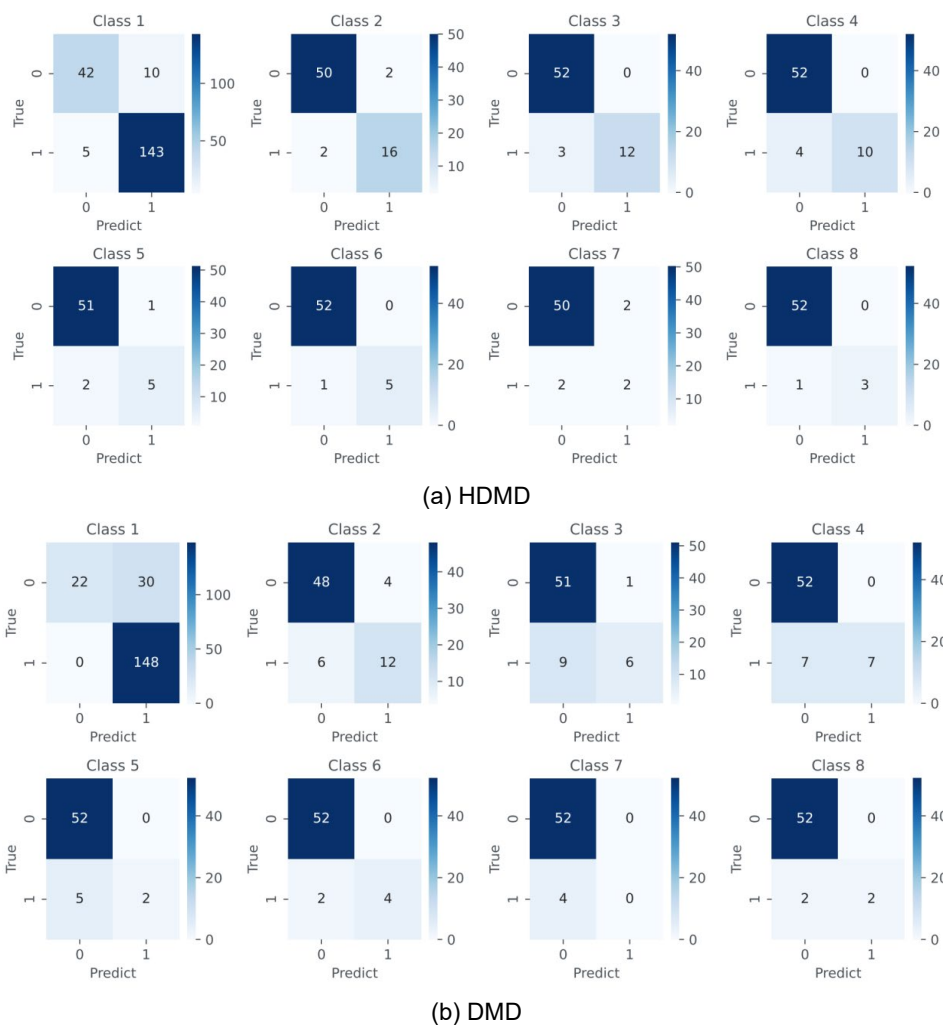


Figure 8. Confusion Matrix Heatmap of HDMD and DMD Classification

Figure 8 shows the classification results of the ECG modal data extracted by the two methods in 8 categories. The darker the diagonal color of the confusion matrix heat map, the better the classification effect. Among them, Figures (a) and (b) correspond to HDMD and DMD modal data respectively, and are confusion matrix heat maps classified in 8 types of abnormal ECG signal data. In category 1, since 148 samples are Myocardial Infarction and 52 samples are healthy controls, they are different from other categories in the heat map. For each category, from the colors of the two squares on the diagonal, it can be seen that the accuracy of HDMD is basically higher than that of DMD. Specific indicators are listed in Table 6.

Table 6. HDMD and DMD modal data classification results

No.	Metric	Accuracy		Precision		Recall		F1 score	
		HDMD	DMD	HDMD	DMD	HDMD	DMD	HDMD	DMD
1	Class 1	0.925	0.85	0.894	1	0.808	0.423	0.848	0.595
2	Class 2	0.943	0.857	0.962	0.889	0.962	0.923	0.962	0.889
3	Class 3	0.955	0.851	0.945	0.85	1	0.981	0.972	0.911
4	Class 4	0.939	0.894	0.929	0.881	1	1	0.963	0.937
5	Class 5	0.949	0.915	0.962	0.912	0.981	1	0.971	0.954
6	Class 6	0.983	0.966	0.981	0.963	1	1	0.990	0.981
7	Class 7	0.929	0.929	0.962	0.929	0.962	1	0.962	0.963
8	Class 8	0.982	0.964	0.981	0.963	1	1	0.990	0.857

Table 6 shows that for the classification effect of modal data extracted by HDMD and DMD, only the 7th category is the same in terms of accuracy, while other HDMD categories are higher, among which the 3rd category is more than 10% higher. In the first category, the Precision of DMD is 10.6% higher than that of HDMD. The other categories are still higher than HDMD. The recall rate is 1.9% and 3.8% lower in categories 5 and 7 respectively. The results of the other categories are similar to those of DMD. Or higher. The F1 score is higher for HDMD in every category, with the highest one being Category 1, which is 25.3% higher than DMD

## Discussion

In this study, we propose a modified HDMD model based on the Hankel matrix for the classification of 12-lead ECG signals. By introducing the Hankel matrix and utilizing the 90% SVR to determine the delay parameters, we effectively solve the rank mismatch problem that occurs when DMD is used directly. Our model shows better performance than traditional DMD methods by calculating mean square error (MSE) and using SVM for binary classification.

Experimental results show that through comparison with DMD, we find that HDMD is better at capturing unstable modes and has significant performance improvements in classification tasks. Specifically, the HDMD model performs better than some existing classification methods in the PTB database. This result is also supported by the performance comparison of various methods in Table 7, which further proves the effectiveness of the HDMD model.

**Table 7.** Comparative Analysis of Classification Algorithms for 12-Lead ECG Signals on the PTB Database

No.	Studies	Method	Classifier	Performance
1	This study	HDMD	SVM	Acc=95.1, Pre=95.2, Rec=96.4, F1=95.7, MSE=0.165
2	This study	DMD	SVM	Acc=90.3, Pre=92.3, Rec=91.6, F1=88.6, MSE=0.152
3	Liu <i>et al.</i> , 2015 [33]	Polynomial function and DWT	J48 decision tree	Acc=94.40
4	Tripathy <i>et al.</i> , 2014 [34]	Principal component multivariate multiscale sample entropy	LS-SVM	Acc=90.34,
5	Al-Yami <i>et al.</i> , 2017 [35]	Histogram-based Features, Two-sample Kolmogorov-Smirnov Test	CART	Acc=94, Sen=96, Spe=92
6	Sharma <i>et al.</i> , 2015 [36]	multiscale energy and eigenspace (MEES)	SVM+KNN	Acc=96.00, Sen=93.00, Spe=99.00, Loc Acc =99.58
7	Scidhar <i>et al.</i> , 2016 [37]	DWT+Nonlinear feature extraction	KNN	Acc=98.80, Sen=99.45, Spe=96.27, Loc Acc: 99.97
8	Lodhi <i>et al.</i> , 2018 [38]	-	CNN	Acc=93.5, Sen=94, Spe=86,
9	Arif <i>et al.</i> , 2012 [39]	DWT	KNN	Sen=99.97, Spe=99.9
10	Sun <i>et al.</i> , 2012 [40]	ST segment polynomial features	LT-MIL	Sen=92.5, Spe=89.1
11	Sharma <i>et al.</i> , 2015 [41]	multi-scale DWT	KNN+ SVM	Acc=96, Sen=93, Spe=99
12	Padhy <i>et al.</i> 2017 [42]	SVD+wavelet energy	SVM	Acc=95.30, Sen=94.6, Spe=96.0

Ac=Accuracy(%), Pre=Precision(%), Rec=Recall(%), F1=F1 score(%), Sen= Sensitivity(%), Spe=Specificity(%), Loc Acc=localization Acc(%)

The SVR plays an important role in determining the delay parameters of the Hankel matrix. By analyzing the SVR, we can effectively select appropriate delay parameters, thereby improving the model's stability and classification performance.

Despite the excellent performance of our model, there are still some limitations. First, although HDMD performs well in binary classification tasks, the accuracy of the model still has room for improvement. Further optimization of model parameters and algorithms can improve classification accuracy. Second, this study mainly focuses on binary classification tasks, and future work needs to explore how to extend the HDMD model to multi-classification problems to handle more heart disease types and provide more comprehensive diagnostic support.

## Conclusion

The research results of this article show that multi-modal decomposition and data reconstruction of ECG signal data, using the constructed Hankel matrix in DMD to perform singular value decomposition and extract modes, can more deeply extract the internal time and space characteristics of data with time series, which helps to further classify ECG data. When using the same SVR, HDMD extracts more modes than DMD, and the eigenvalues basically change continuously. However, the eigenvalues of DMD directly on the original data of the ECG signal are relatively discrete, and richer data information cannot be obtained. At the same time, when the inverse Hankelization operator is used to perform inverse transformation on the extracted Hankel matrix to obtain reconstructed data, the reconstruction error is much smaller than that of DMD, with a difference of about 0.3 on individual data. Finally, by performing SVM classification on the modal data extracted by the two methods, and comparing the classification effects of each category, it was found that HDMD performs much better than DMD in all aspects, with the highest accuracy rate being more than 10% higher. Despite the remarkable results achieved in this study, the small sample size of some categories may have an impact on the generalisation ability of some classification tasks. In addition, the high computational complexity of HDMD, especially in the singular value decomposition and inverse Hankelisation stages, may limit its applicability in real-time applications. Future research could further improve the applicability and computational efficiency of the model through data enhancement, algorithm optimisation or hardware acceleration, while exploring more efficient multi-classification methods for accurate diagnosis of various types of anomalies.

## Conflicts of Interest

The author(s) declare(s) that there is no conflict of interest regarding the publication of this paper.

## Acknowledgement

The authors are grateful to the "Ministry of Higher Education Malaysia for the Fundamental Research Grant Scheme" with Project Code: FRGS/1/2024/STG06/UMS/01/1 for their support in this research.

## References

- [1] Nawaz, S. A., Arshad, M., Aslam, T., Wajid, A. H., Shah, R. A., & Malik, M. H. (2024). ECG Based Heart Disease Diagnosis Using Machine Learning Approaches. *Journal of Computing & Biomedical Informatics*.
- [2] Healio. (n.d.). ECG topic reviews and criteria. Healio. <https://www.healio.com/cardiology/learn-the-heart/ecg-review/ecg-topic-reviews-and-criteria>
- [3] Aggarwal, R., Podder, P., & Khamparia, A. (2022). Ecg classification and analysis for heart disease prediction using xai-driven machine learning algorithms. In *Biomedical data analysis and processing using explainable (XAI) and responsive artificial intelligence (RAI)* (pp. 91-103). Singapore: Springer Singapore.
- [4] Chaugule, V., Duddridge, A., Sikroria, T., Atkinson, C., & Soria, J. (2023). Investigating the linear dynamics of the near-field of a turbulent high-speed jet using dual-Particle Image Velocimetry (PIV) and Dynamic Mode Decomposition (DMD). *Fluids*, 8(2), 73.
- [5] Andreuzzi, F., Demo, N., & Rozza, G. (2023). A dynamic mode decomposition extension for the forecasting of parametric dynamical systems. *SIAM Journal on Applied Dynamical Systems*, 22(3), 2432-2458.
- [6] Huhn, Q. A., Tano, M. E., Ragusa, J. C., & Choi, Y. (2023). Parametric dynamic mode decomposition for reduced order modeling. *Journal of Computational Physics*, 475, 111852.
- [7] Sudhesh, K. M., Sowmya, V., Kurian, S., & Sikha, O. K. (2023). AI based rice leaf disease identification enhanced by Dynamic Mode Decomposition. *Engineering Applications of Artificial Intelligence*, 120, 105836.
- [8] Long, Y., Guo, X. A., & Xiao, T. (2024). Research, Application and Future Prospect of Mode Decomposition in Fluid Mechanics. *Symmetry*, 16(2), 155.
- [9] Colbrook, M. J., Li, Q., Raut, R. V., & Townsend, A. (2024). Beyond expectations: residual dynamic mode decomposition and variance for stochastic dynamical systems. *Nonlinear Dynamics*, 112(3), 2037-2061.
- [10] Ingabire, H. N., Wu, K., Amos, J. T., He, S., Peng, X., Wang, W., ... & Ren, P. (2021). Analysis of ECG signals by dynamic mode decomposition. *IEEE Journal of Biomedical and Health Informatics*, 26(5), 2124-2135.
- [11] Gillard, J., & Usevich, K. (2022). Hankel low-rank approximation and completion in time series analysis and forecasting: a brief review. *arXiv preprint arXiv:2206.05103*.
- [12] Sun, W., Zhou, Y., Xiang, J., Chen, B., & Feng, W. (2021). Hankel matrix-based condition monitoring of rolling element bearings: an enhanced framework for time-series analysis. *IEEE Transactions on Instrumentation and Measurement*, 70, 1-10.
- [13] Frolov, E., & Oseledets, I. (2023). Tensor-based sequential learning via hankel matrix representation for next item recommendations. *IEEE Access*, 11, 6357-6371.
- [14] Orinaitė, U., & Landauskas, M. (2021). Novel feature extraction technique based on ranks of Hankel matrices

- with application for ECG analysis. *Mathematical Models in Engineering*, 7(2), 40-49.
- [15] Sharma, R. R., & Pachori, R. B. (2018). Baseline wander and power line interference removal from ECG signals using eigenvalue decomposition. *Biomedical Signal Processing and Control*, 45, 33-49.
- [16] Curtis, C. W., Jay Alford-Lago, D., Bollt, E., & Tuma, A. (2023). Machine learning enhanced Hankel dynamic-mode decomposition. *Chaos: An Interdisciplinary Journal of Nonlinear Science*, 33(8).
- [17] Kato, Y., & Nakao, H. (2022, December). Data-driven spectral analysis of quantum spin networks with limited access using Hankel dynamic mode decomposition. In *2022 IEEE 61st Conference on Decision and Control (CDC)* (pp. 5141-5148). IEEE.
- [18] Yang, D., Gao, H., Cai, G., Chen, Z., Wang, L., Ma, J., & Li, D. (2021). Synchronized ambient data-based extraction of interarea modes using Hankel block-enhanced DMD. *International Journal of Electrical Power & Energy Systems*, 128, 106687.
- [19] Wang, L., Li, T., Fan, H., Hu, X., Yang, L., & Yang, X. (2023). Application of Hankel Dynamic Mode Decomposition for Wide Area Monitoring of Subsynchronous Resonance. *Energy Engineering*, 120(4), 851-867.
- [20] Nayak, I., Teixeira, F. L., & Burkholder, R. J. (2023). On-the-Fly Dynamic Mode Decomposition for Rapid Time-Extrapolation and Analysis of Cavity Resonances. *IEEE Transactions on Antennas and Propagation*.
- [21] Gillard, J., & Usevich, K. (2022). Hankel low-rank approximation and completion in time series analysis and forecasting: a brief review. *arXiv preprint arXiv:2206.05103*.
- [22] Goldberger, A. L., Amaral, L. A., Glass, L., Hausdorff, J. M., Ivanov, P. C., & Mark, R. G. (2004). PTB Diagnostic ECG Database. *PhysioNet*. [Online] <https://www.physionet.org/content/ptbdb/1.0.0/>. Version, 1(0).
- [23] Subasi, A., & Mian Qaisar, S. (2023). Signal Acquisition Preprocessing and Feature Extraction Techniques for Biomedical Signals. In *Advances in Non-Invasive Biomedical Signal Sensing and Processing with Machine Learning* (pp. 25-52). Cham: Springer International Publishing.
- [24] Jain, A., Raja, R., Srivastava, S., Sharma, P. C., & Gangrade, J. (2024). Analysis of EEG signals and data acquisition methods: a review. *Computer Methods in Biomechanics and Biomedical Engineering: Imaging & Visualization*, 1-26.
- [25] Davies, H. J., Hammour, G., Zylinski, M., Nassibi, A., Stanković, L., & Mandić, D. P. (2024). The Deep-Match Framework: R-Peak Detection in Ear-ECG. *IEEE Transactions on Biomedical Engineering*.
- [26] Zhao, B., Liu, H., Bi, T., & Xu, S. (2024). Synchrophasor Measurement Method Based on Cascaded Infinite Impulse Response and Dual Finite Impulse Response Filters. *Journal of Modern Power Systems and Clean Energy*.
- [27] Mumtaz, F., Khan, T. S., Alqahtani, M., Sher, H. A., Aljumah, A. S., & Almutairi, S. Z. (2024). Ultra High-Speed Fault Diagnosis Scheme for DC Distribution Systems based on Discrete Median filter and Mathematical Morphology. *IEEE Access*.
- [28] Wang, X., & Sun, L. (2022, April). Extracting dynamic mobility patterns by Hankel dynamic modes decomposition. In *The 11th Triennial Symposium on Transportation Analysis*, Mauritius Island.
- [29] Min, G., & Jiang, N. (2024). Data-driven identification and pressure fields prediction for parallel twin cylinders based on POD and DMD method. *Physics of Fluids*, 36(2). <https://doi.org/10.1063/5.0185882>
- [30] Fan, T. W., Ma, Z. S., Ding, Q., Qi, F., & Wang, L. (2023) Recursive dynamic mode decomposition method for output-only identification of time-varying modal parameters. *Journal of Vibration Engineering*.
- [31] Schizas, I. D. (2020). Online data dimensionality reduction and reconstruction using graph filtering. *IEEE Transactions on Signal Processing*, 68, 3871-3886.
- [32] Görtler, J., Hohman, F., Moritz, D., Wongsuphasawat, K., Ren, D., Nair, R., ... & Patel, K. (2022, April). Neo: Generalizing confusion matrix visualization to hierarchical and multi-output labels. In *Proceedings of the 2022 CHI Conference on Human Factors in Computing Systems* (pp. 1-13).
- [33] B. Liu *et al.*, "A novel electrocardiogram parameterization algorithm and its application in myocardial infarction detection," *Comput. Biol. Med.*, vol. 61, pp. 178-184, Jun. 2015.
- [34] Tripathy, R. K., Sharma, L. N., & Dandapat, S. (2014). A new way of quantifying diagnostic information from multilead electrocardiogram for cardiac disease classification. *Healthcare Technology Letters*, 1(4), 98-103.
- [35] Al-Yami, R. R., Alotaiby, T. N., Aljafar, L. M., Alshebeili, S. A., & Zouhair, J. (2017, November). Classification of single-lead ECG signal to normal and abnormal subjects using histogram-based features. In *2017 International Conference on Electrical and Computing Technologies and Applications (ICECTA)* (pp. 1-3). IEEE.
- [36] Sharma, L. N., Tripathy, R. K., & Dandapat, S. (2015). Multiscale energy and eigenspace approach to detection and localization of myocardial infarction. *IEEE transactions on biomedical engineering*, 62(7), 1827-1837.
- [37] Sridhar, C., Acharya, U. R., Fujita, H., & Bairy, G. M. (2016, October). Automated diagnosis of Coronary Artery Disease using nonlinear features extracted from ECG signals. In *2016 IEEE International Conference on Systems, Man, and Cybernetics (SMC)* (pp. 000545-000549). IEEE.
- [38] Lodhi, A. M., Qureshi, A. N., Sharif, U., & Ashiq, Z. (2018, September). A novel approach using voting from ECG leads to detect myocardial infarction. In *Proceedings of SAI Intelligent Systems Conference* (pp. 337-352). Cham: Springer International Publishing.
- [39] Arif, M., Malagore, I. A., & Afsar, F. A. (2012). Detection and localization of myocardial infarction using k-nearest neighbor classifier. *Journal of medical systems*, 36, 279-289.
- [40] Sun, L., Lu, Y., Yang, K., & Li, S. (2012). ECG analysis using multiple instance learning for myocardial infarction detection. *IEEE transactions on biomedical engineering*, 59(12), 3348-3356.
- [41] Sharma, L. N., Tripathy, R. K., & Dandapat, S. (2015). Multiscale energy and eigenspace approach to detection and localization of myocardial infarction. *IEEE transactions on biomedical engineering*, 62(7), 1827-1837.
- [42] Padhy, S., & Dandapat, S. (2017). Third-order tensor based analysis of multilead ECG for classification of myocardial infarction. *Biomedical Signal Processing and Control*, 31, 71-78.